Chemical dynamics versus transport dynamics in a simple model

1999 J. Phys. A: Math. Gen. 32 3717

(http://iopscience.iop.org/0305-4470/32/20/305)

J. Phys. A: Math. Gen. **32** (1999) 3717–3731. Printed in the UK PII: S0305-4470(99)94749-2

Chemical dynamics versus transport dynamics in a simple model

H Lustfeld† and Z Neufeld‡

† Forum Modellierung and Institut für Festkörperforschung, Forschungszentrum Jülich, D 52425 Jülich, Germany

‡ Department of Applied Mathematics and Theoretical Physics, Silver Street, Cambridge CB3 9EW, UK

Received 1 June 1998, in final form 15 February 1999

Abstract. Reaction equations of homogeneously mixed pollutants in the atmosphere can lead to non-stationary periodic solutions. It is important to know how these solutions are modified under the influence of the atmospheric currents. We investigate this question in a very simple one-dimensional model: the reactions are modelled by the brusselator and the currents are represented by a uniform stream with periodic boundary conditions. In the limit of strong currents we again find the homogeneous solutions whereas for weaker currents complicated spatial and temporal patterns emerge. The role of diffusion is also investigated.

1. Introduction

The concentrations of chemical species (e.g. pollutants) in the atmosphere depend on the atmospheric currents and the chemical reactions. Neglecting cloud formation, humidity, ice etc, the governing equation for the concentration fields can be written

$$\frac{\partial}{\partial t}c_i = f_i(c_1 \dots c_n, \boldsymbol{x}, t) - \boldsymbol{v}(\boldsymbol{x}, t) \cdot \nabla c_i + \epsilon_i \Delta c_i \qquad i = 1, \dots, n \tag{1}$$

where the functions f_i describe the chemical reactions and sources, the second term on the right-hand side represents the advection by the atmospheric currents $\boldsymbol{v}(\boldsymbol{x}, t)$ and the last one is the diffusion term.

If the mixing is strong and the chemical components are homogeneously distributed the concentrations c_i are determined by the chemical reactions alone and the equations reduce to ordinary reaction rate equations. The solutions of these reaction equations need not approach a time-independent limit. They can develop a *chemical dynamics* well known from model reaction schemes and laboratory experiments [1]. Periodic fluctuations can also arise in atmospheric chemistry as has recently been shown in a model system containing six pollutants and two pollutant sources [2–4]. A particular feature was the result that concentrations may change by an order of magnitude within a few days.

If the chemical components are not homogeneously distributed the *transport dynamics* needs also to be considered. In the atmosphere the transport of chemical species is dominated by advection and molecular diffusivities are very small. But the advecting velocity field can be decomposed into large-scale winds and a strongly fluctuating small-scale component. The effect of the latter component on the chemical fields is often described by a 'turbulent' diffusion [5–8] with diffusivity parameters much higher than the molecular ones.

0305-4470/99/203717+15$19.50

In this context two questions arise: first, how do the concentrations develop if the transport dynamics is not negligible? We show here, for a very simple model, that the transport dynamics can lead to very rich new phenomena. Second, what is the effect of the diffusion term? We will show in the same model that if there is a *chemical dynamics* then the diffusion is a *singular* perturbation. It has its own timescales that depend sensitively on the strength of the diffusion term.

Previous work has investigated the interaction between fluid transport and chemical dynamics for reactions like $A + B \to C$ or $A + B \to 2B$ in two-dimensional flows [9–12]. Here we consider a simple one-dimensional flow with a set of reactions that allows for time-dependent chemical dynamics in the homogeneous case. The model is described in section 2, in section 3 we discuss its properties without diffusion and in section 4 we concentrate on the role of diffusion. The conclusion ends the paper.

2. The model

The chemical dynamics of our model is described by the well known Brusselator reaction scheme [13]

$$X \to E \qquad X \to Y \qquad 2X + Y \to 3X \tag{2}$$

where the pollutant X partly decays into an inert substance E, partly into a second constituent Y that autocatalytically reacts with X again. For maintaining the chemical reactions a 'pollutant source' is required pouring out pollutants of type X.

In the absence of transport and if the pollutant source is spatially uniform the concentrations c_1 (of X) and c_2 (of Y) are described by the chemical rate equations†

$$\dot{c}_X = S + c_X^2 c_Y - (1 + b)c_X \qquad \dot{c}_Y = bc_X - c_X^2 c_Y \tag{3}$$

where S is the source strength and b represents the ratio between the decay rate of X into pollutant Y and the decay rate of X into inert substances. Depending on the parameters the concentrations converge to a fixed point or limit cycle in the homogeneous case. Typically periodic solutions with sharp peaks occur. They are analogous to those obtained in the simplified tropospheric chemistry model of [2].

To investigate the interaction between the chemical and transport dynamics we consider a point source producing pollutant X that is transported away by a steady flow. If the diffusion is weak the reactions will be mostly concentrated around the streamline containing the point source. Assuming a closed streamline (e.g. around an isolated vortex) we consider a very simple one-dimensional transport dynamics given by a uniform stream on the unit interval and periodic boundary conditions. (By this we neglect the effects arising due to the curvature of the steramline.) Thus, we obtain the following combined reaction transport equations:

$$\begin{aligned} \frac{\partial}{\partial t}c_X &= S\delta(x) + c_X^2 c_Y - (1 + b)c_X - v\frac{\partial}{\partial x}c_X + \epsilon\frac{\partial^2}{\partial x^2}c_X \\ \frac{\partial}{\partial t}c_Y &= bc_X - c_X^2 c_Y - v\frac{\partial}{\partial x}c_Y + \epsilon\frac{\partial^2}{\partial x^2}c_Y \end{aligned} \tag{4}$$

where the source is located at $x = 0$ and we assumed that the diffusivities ϵ are equal for the two constituents‡. Apart from the diffusion constant the equations contain three control parameters, the decay ratio b, the source strength S and the velocity v.

† The reaction rates and further down the length of the streamline have been scaled to unity by proper rescaling of length, time and concentrations.

‡ In a wind field molecular diffusion is negligible compared with turbulent diffusion. In that case ϵ is equal for all constituents. In our paper small ϵ means small turbulent diffusion.

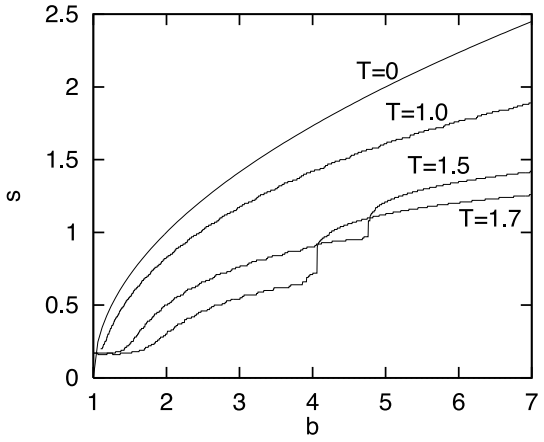

Figure 1. Curves corresponding to the Hopf bifurcation in the parameter plane s–b for different values of the period T.

3. Properties of the model without diffusion

Let us now assume that diffusion is weak and it can be neglected ($\epsilon = 0$). In this case it is convenient to introduce a reference frame co-moving with the flow using a coordinate transformation $\bar{x} = x - vt \bmod 1$. In the moving frame equation (4) reduces to an infinite set of uncoupled pairs of ordinary differential equations, each pair describing the chemical dynamics in individual fluid parcels labelled by their initial coordinate x_0 at time $t = 0$:

$$\begin{aligned} \dot{c}_1 &= s \sum_{n=-\infty}^{\infty} \delta(x_0 + vt + n) + c_1^2 c_2 - (1 + b)c_1 \\ \dot{c}_2 &= bc_1 - c_1^2 c_2. \end{aligned} \tag{5}$$

In the moving frame the point source is moving with a velocity v and the above equation describes a periodically driven (kicked) chemical dynamics with a driving period $T \equiv 1/v$. Note that the phase of the driving depends on the parameter x_0 ($0 < x_0 < 1$) being different for each fluid parcel.

The periodically driven brusselator has been investigated in different contexts considering a constant plus a sinusoidal or delta-function time dependence of the source [14–16]. In the $T \to 0$ limit the normal brusselator is recovered, i.e. very frequent injections correspond to an almost uniform source. In this limit the parameter plane S versus b can be divided into two regions (figure 1): for higher source strengths the concentrations converge to the fixed point $c_1^* = S$, $c_2^* = b/S$. As S is decreased, the fixed point becomes unstable and a Hopf bifurcation occurs along the curve $S = \sqrt{b + 1}$ forming the boundary between the two regions. Below this curve the system converges to a limit cycle, i.e. the concentrations oscillate periodically (figure 2).

When the period T is non-zero but still small ($0 < T \ll 1$), a periodic pulsation with period T of the concentrations appears. Moreover, the initially two-dimensional phase space ($c_1 - c_2$) becomes three dimensional by including the cyclic variable t/T mod 1 and the attractors can be conveniently represented on a stroboscopic section defined by a fixed value of the driving phase.

The dimensionality of the attractor increases as well, and the original fixed point turns to a limit cycle with period T that is a fixed point of the stroboscopic map. Similarly, the original

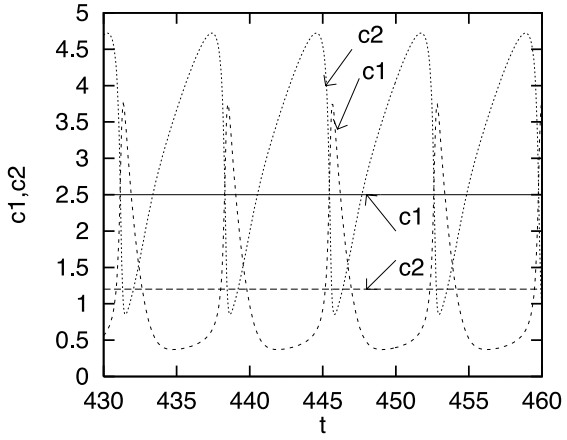

Figure 2. Constant in time and periodic behaviour of the concentrations c_1 and c_2 for the unforced brusselator ($T = 0$). The parameters are $s = 2.5$, $b = 3.0$ and $s = 1.0$, $b = 3.0$, respectively.

limit cycle becomes either (i) a torus corresponding to a quasiperiodic time dependence of the concentrations with one of the periods equal to T (figure 3) or (ii) a periodic orbit with period nT/m, $(n, m = 1, 2, \ldots)$.

This is expected from the characteristic features of periodically driven oscillators. There exist resonant regions for driving frequencies close to their natural frequency multiplied by a rational number. These resonant regions appear here in the parameter space below the Hopf bifurcation curve and are analogous to the Arnold tongues of the so-called 'circle map' [17] (figures 4 and 5). Another effect of the periodic forcing term is that the Hopf bifurcation curve moves to smaller values of S as T increases (figure 1). Since the dynamics is given by a set of two non-autonomous ordinary differential equations chaotic behaviour is also possible for certain values of the parameters leading to a strange attractor in the stroboscopic section (figure 6).

Next we consider the *spatial distribution* of the concentrations in the case of different temporal dynamics. The spatial dependence can be reconstructed from the temporal dynamics by taking into account the phase shift of the driving for different fluid parcels and the possibly different initial conditions.

(α) *Periodic time dependence with period T.*

This behaviour occurs for large T (i.e. small velocities of the flow). In this case the concentrations oscillate and the phase of the oscillations is given by the phase of the driving t/T mod 1. Thus the final state is independent of the initial conditions. In the moving frame the only difference in the periodic time dependence at different points of the flow is a time lag $\bar{x}T$

$$c(\bar{x}, t) = c(t + \bar{x}T; x_0 = 0) \tag{6}$$

that corresponds to a non-uniform but time-independent distribution in the standing frame $c(x, t) = c(xT; x_0 = 0)$.

(β) *Periodic oscillations with period nT.*

This behaviour is characteristic to the resonant regions. The concentrations at each time can take one of the n possible values depending on the initial conditions

$$c(\bar{x}, t) \in \{c(t + iT + \bar{x}T; x_0 = 0)\} \qquad i = 0, \ldots, n-1 \tag{7}$$

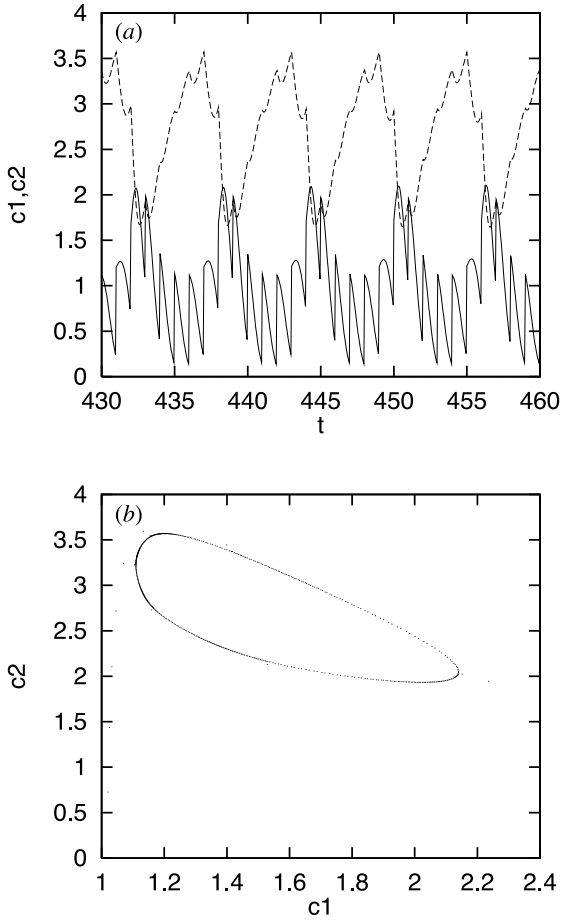

Figure 3. Quasiperiodic time dependence of the concentrations c_1 and c_2 (*a*), and stroboscopic section (*b*) for $s = 1.0$, $b = 3.0$ and $T = 1.0$.

where the value of integer i is a function of the coordinate $\bar{x}$ due to its dependence on the initial concentrations $c(\bar{x}, t = 0)$. The boundary between the basins of attraction of the n branches of the solution is a twisted (Möbius-type) surface in the phase space, so that the basin of attraction of branch i becomes the basin of attraction of branch $i + 1 \bmod n$ after one period T. Thus any smooth initial condition must have at least one intersection with this surface. At this point the concentrations converge to two different branches and a discontinuity appears in the spatial dependence of the concentrations (figure 7). Note that this jump is not a consequence of the delta function in equation (5) but due to geometrical constraints. An initially random distribution can lead to a completely staggered distribution whose envelopes are the n branches of the solution. The jumps stay at fixed positions in the moving reference frame.

(γ) *Quasiperiodic time dependence*.

This is present below the Hopf bifurcation curve between the resonances and dominates for small T because with increasing T the region below the Hopf curve shrinks and at the same time the resonant islands grow in size. This case corresponds to a motion on a torus in the phase space. The dynamics can be characterized by two cyclic angle-like variables, one of them is the phase of the driving and the other one depends smoothly on the initial concentrations:

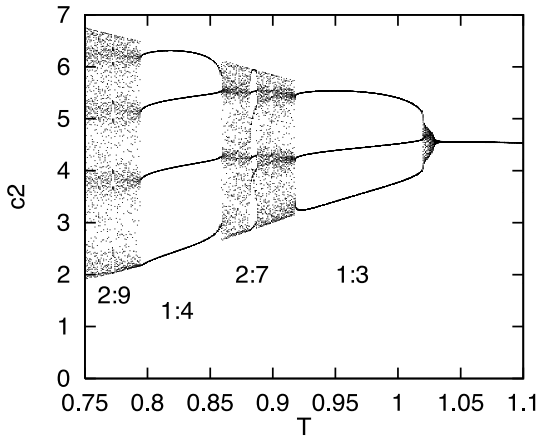

Figure 4. Stroboscopic plot of c_2 as function of T for $s = 1.9$ and $b = 7.7$. The Hopf bifurcation occurs around $T = 1.03$ and there are resonant windows inside the quasiperiodic region labelled by the ratio of the two periods.

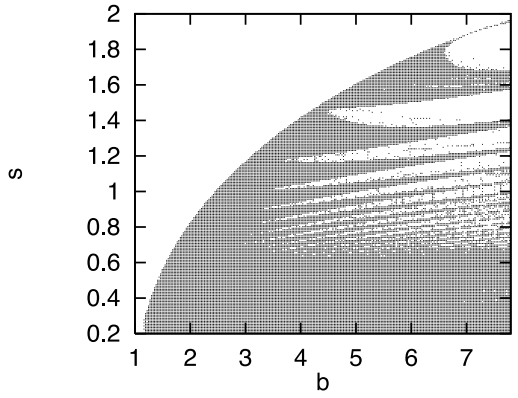

Figure 5. Periodic (blank) and quasiperiodic (grey) regions in a section of the parameter space for $T = 1.0$. The behaviour of the system was identified by calculating the leading Lyapunov exponent which is smaller than -0.0025 for the blank region.

$c(\bar{x}, t) = c(t + \tau(\bar{x}); x_0 = 0)$. Therefore, an initially smooth distribution remains smooth in $\bar{x}$ for all times (except at the initial position of the source where the time lag of the source term by T leads to a discontinuity).

(δ) *Chaotic time dependence*.

In this case the time dependence is very sensitive to the initial conditions and thus the distribution becomes irregular on each scale regardless how smooth the initial distribution may have been (figure 9(*a*)).

4. The role of diffusion

Without diffusion the final distributions (except those with the period T) have infinite degeneracy due to an arbitrary uneven† number of jumps. Therefore diffusion is a *singular*

† We do not count the strong increase of the c_1 concentration due to the δ-function shape as a jump.

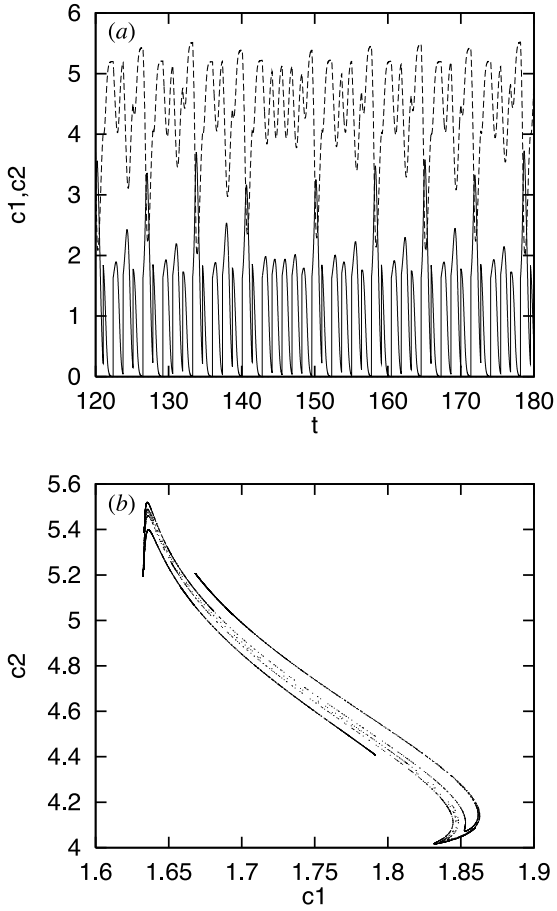

Figure 6. Chaotic time dependence of the concentrations c_1 and c_2 and the stroboscopic section of the strange attractor. The parameters are $s = 1.2$, $b = 7.0$ and $T = 1.36$.

perturbation that has significant consequences for the system even for small ϵ. (For the following computations we used the Crank–Nicholson scheme combined with operator splitting [18].)

We discuss first the simplest nontrivial case of equation (7), which occurs for period $2T$. We denote with a $-+$ ($+-$) jump an 'upward' ('downward') steep increase (decrease) of the concentration, but exclude the strong increase of c_1 at the location of the source. If the diffusion is small enough we can treat a jump as isolated (for a very long time). We find that due to diffusion the jumps move with a drift velocity relative to the flow, (cf figure 7). Scaling and symmetry arguments suggest that this should be proportional to a higher power of $\sqrt{\epsilon}$ and in fact we find numerically a dependence $\propto \epsilon$. The important point, however, is that, averaged over $2T$, each isolated jump moves with the *same* drift velocity. (In fact after time T a $-+$ jump becomes a $+-$ jump and vice versa.) What we expect then as the essential ingredient of equation (7) is that f tries to enforce solutions with a period of $2T$. In appendix A we have derived a simple function f that has just this property *and* makes it possible to treat equation (7) analytically. We then find: first, for times

$$T_1 = \mathcal{O}(1) \tag{8}$$

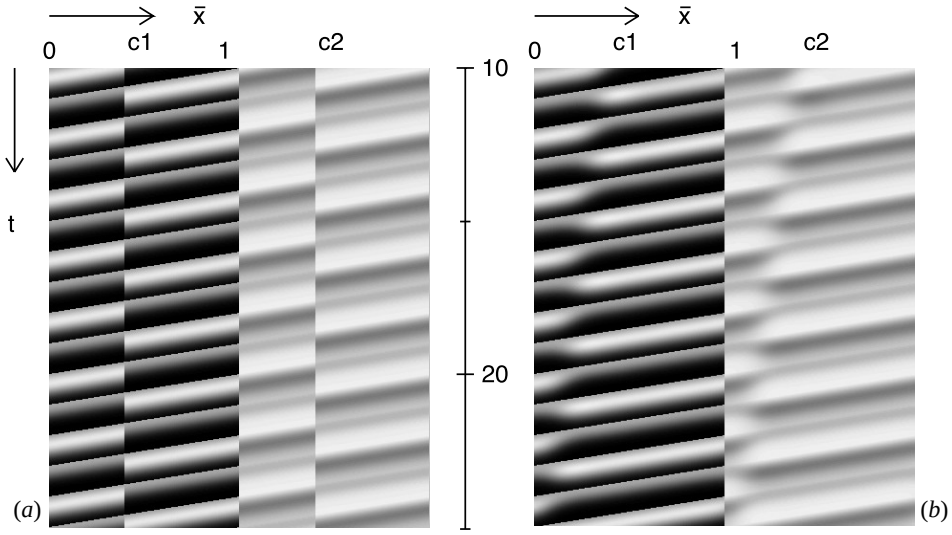

Figure 7. Spatiotemporal plot of the concentrations c_1 (*a*) and c_2 (*b*) along the streamlines in the co-moving frame represented on a greyscale, so that concentrations increase from black to white. The simulation was started with both concentrations equal to zero and the initial position of the source is at $x = 0.2$. Parameters are $s = 1.0$ $b = 5.0$ and $T = 1.7$ In case (*a*) $\epsilon = 0$ and a non-moving discontinuity is present at $x = 0.2$. When diffusion is switched on $\epsilon = 0.001$ the discontinuity becomes rounded and moves (to the left in this case) along the streamline.

all jumps with distance of $\mathcal{O}(\sqrt{\epsilon})$ vanish. During this time the effect of the diffusion is just a coarse graining. Second, over a period of about

$$T_2 = \mathrm{e}^{\beta/\sqrt{\epsilon}} \qquad \beta = \mathcal{O}(1) \tag{9}$$

all other jumps are affected. The diffusion gradually removes the degeneracies, until a final state emerges that has no jumps at all, besides the generic one that cannot be removed. In our model this state has global stability. Numerically we find the same phenomena for the brusselator, cf figure 7(*b*).

The effects described here occur quite independently of how small ϵ is. On the other hand T_2 depends exponentially on $1/\sqrt{\epsilon}$. When a further perturbation has to be added acting on a timescale τ we expect quite different situations depending on whether $T_2 > \tau$ or $T_2 < \tau$. This means that the effect of such a perturbation depends *sensitively* on $\sqrt{\epsilon}$.

We expect even more complicated properties of the concentrations having higher periods (in absence of diffusion). There are two reasons: (i) if the period is nT the system has at any location $n - 1$ choices for the height of a jump, (ii) the jumps are no longer equivalent but are separated in classes and only jumps within the *same* class change into each other and therefore move with the same mean drift velocity v_d. Indeed, the effect of diffusion on the periodic solution can in some cases be very significant, leading to a complicated irregular behaviour of the system in space and time. As can be seen from figure 8, inside the chaotic concentration field coherent regions with regular periodic time dependence appear and disappear continuously. This kind of spatiotemporal intermittency has been observed in different extended systems [19, 20]. If the initial distribution is smooth first at least the intrinsic jump appears as described above. The pertubation of the periodic solution around the discontinuity leads to a chaotic time dependence which due to the diffusive coupling spreads over the whole system. Such behaviour can be observed for parameters which lie in the vicinity of the chaotic regimes of

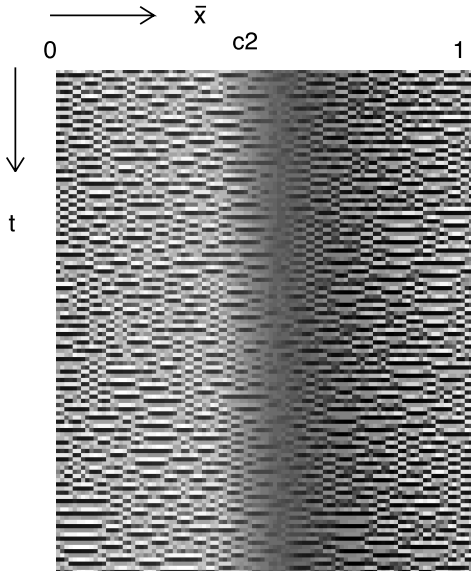

Figure 8. Stroboscopic spatiotemporal plot of concentration c_2 for parameters $s = 0.8$, $b = 6.0$ and $T = 1.85$, corresponding to a periodic behaviour with period $3T$ when diffusion is neglected. Here $\epsilon = 2 \times 10^{-5}$ leads to an irregular spatiotemporal dynamics.

the $\epsilon = 0$ case. The solution appears already for very small ϵ demonstrating that the system is sensitive to weak diffusion.

In case of quasiperiodic local behaviour, instead of a finite number of discrete branches, a continuous set of solutions exists filling the torus in the phase space. Thus the discontinuity present in the case without diffusion is easily removed by an arbitrarily weak diffusion leading to almost coherent quasiperiodic oscillations of the whole system.

When the parameters correspond to chaotic local dynamics, diffusion tends to form intermittent correlated regions of finite extent in space and time (figure 9). As ϵ is increased, the local dynamics becomes completely regular with a frozen irregular distribution in space which certainly depends on the initial distribution.

5. Conclusion

High peaks can appear in periodic solutions of chemical reaction equations in which the constituents are *homogeneously* mixed tracer gases of the atmosphere. However, depending on the motion of the fluid the mixing need not be homogeneous at all, and the question arises how these solutions will then change.

In this paper we investigate this question for a simple model, the brusselator with pointlike source in a one-vortex flow. Simple as the model appears, it demonstrates the strong modifications occurring as soon as we move away from the homogeneous situation. One observes this when computing the concentration distribution along the (closed) streamline in which the source is located. As a function of time we detect solutions that are very similar to those of the homogeneous case. This happens as long as the period T of the flow is small. Furthermore, we find solutions with period nT, moreover quasiperiodic and chaotic ones. All these solutions, (except that with period T) are infinitely degenerate and therefore depend on the initial distribution. Even if the latter is smooth, the distributions can asymptotically have

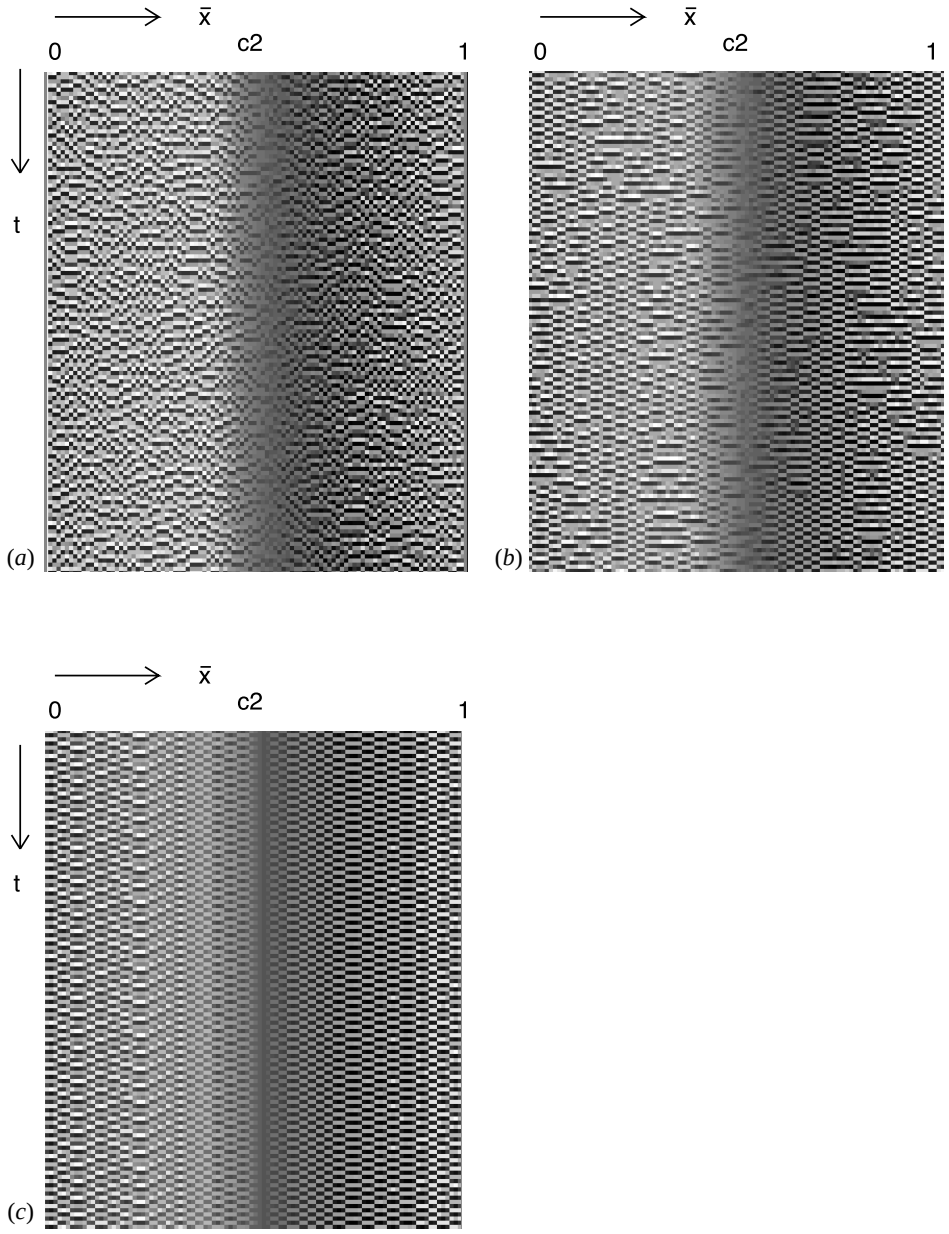

Figure 9. Stroboscopic spatiotemporal plots of concentration c_2 for $s = 0.8$, $b = 6.0$ and $T = 1.89$. These parameters correspond to a chaotic local dynamics when diffusion is not considered. We assumed that the initial concentrations are randomly distributed in a small interval [0, 0.0001] for both constituents. The diffusion coefficient is $\epsilon = 0$ (*a*), $\epsilon = 1.5 \times 10^{-5}$ (*b*) and $\epsilon = 2 \times 10^{-5}$ (*c*), respectively.

an arbitrary (uneven) number of discontinuities, in the chaotic case on *all scales*.

In such situations diffusion is a singular perturbation and switching on arbitrary small diffusion along the streamline has two effects: first after a time of $\mathcal{O}(1)$ it leads to a 'coarse graining' of the distribution on a space scale $\propto \sqrt{\epsilon}$ where ϵ is the strength of the diffusion.

Second, on a timescale $\propto \mathrm{e}^{\sqrt{\beta}/\sqrt{\epsilon}}$, ($\beta = \mathcal{O}(1)$), it removes all discontinuities but one for solutions which have (without diffusion) period $2T$. This shows that the solutions depend sensitively on $\sqrt{\epsilon}$. For parameters that lead (without diffusion) to solutions of higher period, quasiperiodic or chaotic time dependence the coupling of the local dynamics leads to more complex and irregular spatio-temporal patterns. All these solutions have nothing in common with the case of homogeneous mixing we started with.

Although this one-dimensional model is far from being a realistic representation of the chemistry and transport in the atmosphere, it shows that even a trivial non-turbulent flow interacting with a simple but time-dependent chemical dynamics of just two reactants can lead to a complex irregular behaviour of the concentration fields.

Acknowledgments

This work has been supported in part by the German–Hungarian Scientific and Technological Cooperation *classical and quantum chaos and applications*. ZN would like to thank the group of the modelling forum for their kind hospitality at the research center Jülich where part of this work was done. We thank Gert Eilenberger and Tamás Tél for useful discussions.

Appendix A

In this appendix we derive the properties of equation (1) for our model assuming that without diffusion the solution has a $2T$ period in the moving system. We have

$$\partial_t \boldsymbol{c} = \boldsymbol{f}(\boldsymbol{c}, \bar{x}, t) + \epsilon \partial_{\bar{x}}^2 \boldsymbol{c} \tag{A.1}$$

with the periodic boundary conditions

$$\boldsymbol{c}(\bar{x}, t) = \boldsymbol{c}(\bar{x} + 1, t) \qquad \partial_{\bar{x}} \boldsymbol{c}(\bar{x}, t) = \partial_{\bar{x}} \boldsymbol{c}(\bar{x} + 1, t). \tag{A.2}$$

This equation holds true in the frame moving with a velocity $v = 1/T$.

The use of $\boldsymbol{c}$ can be awkward since the components have to be positive. Therefore we write

$$\boldsymbol{n} = \boldsymbol{c} + \text{const} \tag{A.3}$$

and get the equation for $\boldsymbol{n}$

$$\partial_t \boldsymbol{n} = \boldsymbol{g}(\boldsymbol{n}, \bar{x}, t) + \epsilon \partial_{\bar{x}}^2 \boldsymbol{n} \qquad \text{with} \quad \boldsymbol{g}(\boldsymbol{n}, \bar{x}, t) = \boldsymbol{f}(\text{const} + \boldsymbol{n}, \bar{x}, t) \tag{A.4}$$

and the periodic boundary conditions

$$\boldsymbol{n}(\bar{x}, t) = \boldsymbol{n}(\bar{x} + 1, t) \qquad \partial_{\bar{x}} \boldsymbol{n}(\bar{x}, t) = \partial_{\bar{x}} \boldsymbol{n}(\bar{x} + 1, t). \tag{A.5}$$

Without diffusion $\boldsymbol{n}$ moves exponentially fast to its asymptotic limit $\boldsymbol{n}^{(0)}$ having the properties

$$\begin{aligned} &\boldsymbol{n}^{(0)}(\bar{x}, t) = \boldsymbol{n}^{(0)}(\bar{x}, t + 2T) \\ &\text{and either} \\ &\boldsymbol{n}^{(0)}(\bar{x}, t) = \boldsymbol{n}^{(0)}(t - \bar{x}T) \\ &\text{or} \\ &\boldsymbol{n}^{(0)}(\bar{x}, t) = \boldsymbol{n}^{(0)}(T + t - \bar{x}T) \end{aligned} \tag{A.6}$$

$n^{(0)}$ and its properties also remain important if diffusion is switched on since g can be expanded around $n^{(0)}$.

To understand the physics of equation (A.4) with the conditions of equation (A.6) we construct a simple model for the function g in three steps.

Step 1. We introduce a very simple $\boldsymbol{n}^{(0)}$

$$n_1^{(0)}(\bar{x},t) = \mathrm{Re}\,\{a\mathrm{e}^{\mathrm{i}\pi(t/T-\bar{x})}\} \qquad n_2^{(0)}(\bar{x},t) = \mathrm{Im}\,\{a\mathrm{e}^{\mathrm{i}\pi(t/T-\bar{x})}\} \tag{A.7}$$

and we represent the two-dimensional vectors by complex numbers.

Step 2. We use the ansatz

$$n(\bar{x},t) = \mathrm{e}^{\mathrm{i}\pi(t/T-\bar{x})}\cdot m(\bar{x},t) \tag{A.8}$$

and get the partial differential equation for m

$$\partial_t m = \tilde{g} - \mathrm{i}\pi\epsilon\partial_{\bar{x}}m - \pi^2\epsilon m + \epsilon\partial_{\bar{x}}^2 m \qquad \text{with}$$
$$\tilde{g} = \mathrm{e}^{-\mathrm{i}\pi(t/T-\bar{x})}g(\mathrm{e}^{\mathrm{i}\pi(t/T-\bar{x})}m,\bar{x},t) - (\mathrm{i}\pi/T)m. \tag{A.9}$$

The terms $\mathrm{i}\pi\epsilon\partial_{\bar{x}}m$ and $\pi^2\epsilon m$ are of higher order in $\sqrt{\epsilon}$ and will be left out for simplicity. The boundary conditions of equation (A.5) are replaced by

$$m(\bar{x},t) = -m(\bar{x}+1,t) \qquad \partial_{\bar{x}}m(\bar{x},t) = -\partial_{\bar{x}}m(\bar{x}+1,t). \tag{A.10}$$

Step 3. We construct a simple $\tilde{g}$. Because of equation (A.7) and (A.8) $m^{(0)}$ can only take two values,

$$m^{(0)} = \pm a \tag{A.11}$$

and a can be chosen to be real and positive. When m is in the neighbourhood of $m^{(0)}$ $\tilde{g}$ can be expanded and we obtain

$$\tilde{g} = -\alpha(\bar{x},t)(m-a)+\cdots \qquad \text{or} \qquad \tilde{g} = -\alpha(\bar{x},t)(m+a)+\cdots. \tag{A.12}$$

For $\alpha(\bar{x},t)$ we insert a real positive constant†. The linear approximation of $\tilde{g}$ is of course incorrect if m is not close to $\pm a$. A nonlinearity is simply added by the prescription

$$\tilde{g} = \begin{cases} -\alpha(m-a) & \text{for} \quad |m-a| < |m+a| \\ -\alpha(m+a) & \text{else.} \end{cases}$$

Thus we get the partial differential equation:

$$\partial_t m = \tilde{g} + \epsilon\partial_{\bar{x}}^2 m \qquad \text{with} \quad \tilde{g} = \begin{cases} -\alpha(m-a) & \text{for} \quad \mathrm{Re}\,m > 0 \\ -\alpha(m+a) & \text{for} \quad \mathrm{Re}\,m \leqslant 0. \end{cases} \tag{A.13}$$

Boundary conditions are given by equation (A.10). The connection between n and m is given by equation (A.8) and the real and imaginary part of n are the components of $\boldsymbol{n}$.

A.1. Properties of the solutions of equation (A.13)

(I) Diffusion switched off, i.e. $\epsilon = 0$.
m consists asymptotically of an uneven number of jumps with values $\pm a$. The number of jumps can be arbitrarily high and is determined exclusively by the initial distribution of m.

(II) Diffusion switched on, i.e. $\epsilon > 0$.

† α could be a complex constant as well as long as the real part is positive.

(1) Isolated jump.

We assume that there is a constant velocity $\sqrt{\epsilon}w$ with which the jump is moving. Transforming to new coordinates y with

$$\bar{x} = y + \sqrt{\epsilon}wt \tag{A.14}$$

and assuming that the jump occurs at $y = 0$ the two equations are to be solved:

$$\begin{aligned} 0 &= -\alpha(m + a) + \sqrt{\epsilon}w\partial_y m + \epsilon\partial_y^2 m \qquad y < 0 \\ 0 &= -\alpha(m - a) + \sqrt{\epsilon}w\partial_y m + \epsilon\partial_y^2 m \qquad y > 0. \end{aligned}$$

Because of the boundary conditions for the isolated jump

$$m(-\infty) = -a \qquad m(\infty) = a$$

the solution is

$$\begin{aligned} m_-(y) &= A\mathrm{e}^{\gamma y/\sqrt{\epsilon}} - a \qquad \gamma = (\tfrac{1}{2})\left(-w + \sqrt{4\alpha + w^2}\right) \qquad y \leqslant 0 \\ m_+(y) &= B\mathrm{e}^{\tilde{\gamma} y/\sqrt{\epsilon}} + a \qquad \tilde{\gamma} = (\tfrac{1}{2})\left(-w - \sqrt{4\alpha + w^2}\right) \qquad y \geqslant 0 \end{aligned} \tag{A.15}$$

with the boundary condition

$$m_-(0) = m_+(0) \qquad m'_-(0) = m'_+(0).$$

Because of equation (A.13) there is the further condition

$$\mathrm{Re}\,\{m_-(0)\} = 0.$$

Therefore $A = a$ and $B = -a$, m is real and the condition for w is obtained from

$$a\gamma = -a\tilde{\gamma}$$

which means

$$w = 0.$$

(2) Two interacting jumps isolated from the rest.

Let the $-+$ jump be left, the $+-$ jump be right. Both jumps move because of an interaction with each other and we assume that the interaction changes the speed and shape of the jumps only slowly (the distance $2x_d$ between them decreases of course).

First, we rescale to avoid the ϵ dependence

$$\xi = \frac{\bar{x}}{\sqrt{\epsilon}}. \tag{A.16}$$

Next we transform into a coordinate system moving with the $-+$ jump, whose position is at 0. We obtain

$$\xi = \eta + w_d t \tag{A.17}$$

and

$$\begin{aligned} 0 &= -\alpha(m_- + a) + w_d\partial_\eta m_- + \partial_\eta^2 m_- \qquad \eta \leqslant 0 \\ 0 &= -\alpha(m_+ - a) + w_d\partial_\eta m_+ + \partial_\eta^2 m_+ \qquad \eta \geqslant 0. \end{aligned} \tag{A.18}$$

Boundary conditions are

$$m_-(-\infty) = -a \qquad m_-(0) = m_+(0) \qquad m'_-(0) = m'_+(0). \tag{A.19}$$

Furthermore, the presence of the $+-$ jump is taken care of by the condition

$$m'_+(\xi_d) = 0 \tag{A.20}$$

and we have the constraint (cf equation (A.13))

$$\mathrm{Re}\,\{m_-(0)\} = 0. \tag{A.21}$$

Then we get with an exponential ansatz (cf equation (A.15)

$$\begin{aligned} m_-(\eta) &= A\mathrm{e}^{\gamma\eta} - a \qquad \eta \leqslant 0 \\ m_+(\eta) &= B\mathrm{e}^{\tilde{\gamma}\eta} + C\mathrm{e}^{\gamma\eta} + a \qquad 0 \leqslant \eta \leqslant \xi_d. \end{aligned} \tag{A.22}$$

Again, m can be chosen to be real and the conditions equations (A.19)–(A.21) yield

$$\begin{aligned} A - a &= B + C + a \qquad A\gamma = B\tilde{\gamma} + C\gamma \\ 0 &= B\tilde{\gamma}\mathrm{e}^{\tilde{\gamma}\xi_d} + C\gamma\mathrm{e}^{\gamma\xi_d} \qquad A - a = 0. \end{aligned} \tag{A.23}$$

From these equations we get w_d (neglecting all terms w_d^2 and higher)

$$w_d \approx 2\sqrt{\alpha}\mathrm{e}^{-2\sqrt{\alpha}\xi_d} \tag{A.24}$$

which is correct for

$$\sqrt{\alpha}\xi_d > 1. \tag{A.25}$$

From scaling arguments we infer that equation (A.25) gives the correct order of magnitude for $\sqrt{\alpha}\xi_d < 1$.

One can also use equation (A.24) to prove that there is no stationary state. If it were all the equations would be exact and in particular equation (A.24) which would in turn be a contradiction.

Now we compute the lifetime t_l of a jump which is in the original coordinates

$$t_l = \frac{1}{4\alpha}(\mathrm{e}^{2\sqrt{\alpha}x_d/\sqrt{\epsilon}} - 1). \tag{A.26}$$

(3) n interacting jumps.

To treat this problem we take into account the interaction between nearest neighbours only (the interaction between next nearest neighbours is exponentially small compared to the interaction between the nearest neighbours). Then it is sufficient to look into the problem of one jump between two other jumps. We approximate the interaction again by boundary conditions and obtain two conditions of the form equation (A.20). Performing an analogous computation with the same approximations we obtain for the velocity of the jump

$$w_d \approx 2\sqrt{\alpha}(\mathrm{e}^{-2\sqrt{\alpha}x_{d+}/\sqrt{\epsilon}} - \mathrm{e}^{-2\sqrt{\alpha}x_{d-}/\sqrt{\epsilon}}). \tag{A.27}$$

Here $2x_{d+}$ ($2x_{d-}$) is the distance to the right (left) jump. From this result we conclude that all states with more than one jump will be unstable since two neighbouring jumps will annihilate each other.

References

[1] Scott S K 1991 *Chemical Chaos* (Oxford: Oxford University Press)

[2] Poppe D and Lustfeld H 1996 *J. Geophys. Res.* **101** 14 373

[3] Krol M and Poppe D 1999 *J. Atmos. Chem.* **29** 1

[4] Lustfeld H 1998 Instabilities of pollutant concentrations in the atmosphere due to chemical reactions *A Perspective Look at Nonlinear Media in Physics, Chemistry and Biology* ed J Parisi, S C Müller and W Zimmermann (Berlin: Springer)

[5] Csanady G T 1973 *Turbulent Diffusion in the Environment* (Dordrecht: Reidel)

[6] Monin A S and Yaglom A M 1973 *Statistical Fluid Dynamics: Mechanics of Turbulence* vol 1, 2nd edn (Cambridge, MA: MIT Press)

[7] Panchev S 1985 *Dynamic Meteorology* (Dordrecht: Reidel)

[8] Nester K, Panitz H-J and Fiedler F 1995 *Meteorol. Atmos. Phys.* **57** 201, and references therein

[9] Sokolov I M and Blumen A 1991 *Int. J. Mod. Phys.* B **5** 3127
[10] Metcalfe G and Ottino J M 1994 *Phys. Rev. Lett.* **72** 2875
[11] Reigada R, Sagués F, Sokolov I M, Sancho J M and Blumen A 1997 *Phys. Rev. Lett.* **78** 741
[12] Toroczkai Z, Károlyi Gy, Péntek Á, Tél T and Grebogi C 1998 *Phys. Rev. Lett.* **80** 500
[13] Haken H 1983 *Synergetics, an Introduction* (Berlin: Springer)
[14] Schreiber I *et al* 1988 *Phys. Lett.* A **128** 66
[15] Kai T and Tomita K 1979 *Prog. Theor. Phys.* **61** 54
[16] Aronson D G *et al* 1986 *Phys. Rev.* A **33** 2190
[17] Ott E 1993 *Chaos in Dynamical Systems* (Cambridge: Cambridge University Press)
[18] Press W H *et al* 1992 *Numerical Recipies in C* (Cambridge: Cambridge University Press)
[19] Kaneko K 1984 *Prog. Theor. Phys.* **72** 480
[20] Chatè H and Maneville P 1988 *Physica* D **32** 409